Front. Chem. Sci. Eng. 2020, 14(1): 41–52
https://doi.org/10.1007/s11705-019-1796-1

RESEARCH ARTICLE

Near-infrared fluorescent probe for fast track of cyclooxygenase-2 in Golgi apparatus in cancer cells

Bhaskar Gurram[1], Miao Li[1], Jiangli Fan[1], Jingyun Wang[2], Xiaojun Peng (✉)[1]

1 State Key Laboratory of Fine Chemicals, Dalian University of Technology, Dalian 116024, China
2 School of Life Science and Biotechnology, Dalian University of Technology, Dalian 116024, China

Abstract Cyclooxygenase-2 (COX-2) has been used as an excellent traceable biomarker, and exists maximally in Golgi apparatus (Cancer cells). Celecoxib (CCB) is a selective inhibitor for COX-2, and has been used as one of non-steroidal anti-inflammatory drug. Herein we report the conjugation of nile blue (NB) with CCB via a six-carbon linkage to form a fluorescence probe NB-C6-CCB for the detection of COX-2. NB-C6-CCB displays strong fluorescence with the emission peak centered at near-infrared wavelength (700 nm) in tumor cells or tumor tissues with high expression of COX-2. Importantly, NB-C6-CCB can discriminate cancer cells (MCF-7) fluorescence intensity from normal ones (COS-7) in the co-culture medium under confocal microscope. Subcellular localization of the NB-C6-CCB preferentially points to the Golgi apparatus and increases the fluorescent intensity. The competitive analysis (with CCB) and Native-PAGE analysis confirmed that NB-C6-CCB shows selective binding affinity towards COX-2 enzyme. Competitive analysis with CCB (flow cytometry assay) revealed the fluorescence intensity fluctuation due to pretreatment of CCB with different concentrations, indicating that the NB-C6-CCB is a precise or sensitive probe for the COX-2. Tumor tissue (depth: 500 μm), organs and mice imaging tests show excellent near-infrared visualization, specific localization and identification of tumors.

Keywords cyclooxygenase-2, nile blue, CCB, Golgi apparatus, NIR imaging

1 Introduction

Cancer is a deadly disease worldwide and mortality of cancer patients is increasing every year. Presently, multiple biomedical imaging techniques are used in all phases of cancer management or treatment, such as magnetic resonance imaging (MRI), single-photon emission computed tomography and X-ray imaging. These techniques are essential part of cancer clinical protocols and are able to provide morphological, structural, metabolic and functional information. However, these techniques detect absolute or above stages of cancers and requires expensive instruments [1–5]. During the cancer treatment, the localization, deep tissue penetration and selectivity of tumors are crucial factors [6,7]. Hence, selecting a fluorescent probe with long wavelength, especially near-infrared (NIR) above 650 nm), is an important approach, which features deep tissue penetration without toxicity towards living normal cells [8–11].

Golgi apparatus plays essential roles in the cellular activities as a stress sensor, apoptosis generator, lipid and protein converter, mitotic checkpoint and mediator of malignant transformation in most types of cancer cells. In addition, Golgi produces elevated level of proteins or enzymes in prostate cancer compared to normal cells or tissues. Anticancer drugs (actinomycin D and vinblastine) have been used to disrupt and sensitize the function of protein, which is necessary for the homeostasis of the Golgi apparatus, and Golgi is emerging as a new therapeutic target in prostate cancer and its future target for chemotherapy [12–16]. Hence, organelles (Golgi, endoplasmic reticulum, lysosomes, and nucleus) targeting or localization probes are necessary for advanced cancer imaging and therapy.

Fluorescent probes have been prepared to detect enzymes in cancer cells, due to the unbalanced presence of enzymes in all stages of cancer and the maximum types of tumors [17–19]. Fluorescence turn-on probes designed specifically for glutamyl-transpeptidase, β-galactosidase (β-gal), nitroreductase quinoneoxido-reductase isozyme-1 and cyclooxygenase-2 (COX-2) were used to distinguish

Received August 23, 2018; accepted November 4, 2018

E-mail: pengxj@dlut.edu.cn

cancer cells from normal cells [17,20–24]. Correspondingly, the fluorescence imagining of COX-2 in Golgi apparatus of cancer cells and the discrimination of cancer from both the inflammation and normal tissues were demonstrated [8,19,25]. Celecoxib (CCB) conjugated fluorescent probe for discriminate cancer cells (MCF-7) from normal cells (COS-7) in the single culture medium under confocal microscope has been reported recently in our group [26]. NIR "off-on" fluorescence probes for excellent imaging via targeting Pim-1 kinase and KIAA1363 in cancer cells have also been reported in our group [27,28].

COX-2 frequently presents in cancer cells including breast cancer, prostate cancer, gastric cancer, lung tumors, and colon adenocarcinoma but much less in normal cell [29–32]. COX-2 highly expressed in fluorescent probes, conjugated with indomethacin and CCB have been used to discriminate the cancer cells from the inflammation and normal cells were reported in our group [8,19,26].

CCB derivatives have been synthesized as a more selective inhibitor towards COX-2 [33,34]. CCB has superior selectivity to COX-2 than indomethacin (IMC) [34,35]. As a recognition group, the IC_{50} value of indomethacin derivatives is approximately 0.75 μmol/L [8,18]. CCB (IC_{50} = 0.07 μmol/L) shows greater selectivity towards COX-2 with anti-cancer effect [17,34,36]. CCB reduces the viability of H22 cells in a dose and timedependent manner and induces apoptosis in mouse liver cancer cells via the mitochondria-dependent pathway [37]. Polyamine naphthalimide co-treated with CCB to induce the apoptosis in COX-2 over-expressed cells (HT29, Caco-2) has been specified [38].

Herein, we linked CCB as the recognition group with a near infra nile blue (NB) dye as the reporter via a flexible 6-carbon chain to construct a specific red emitting fluorescent probe, NB-C6-CCB (Fig. 1). We assumed that NB-C6-CCB could perform with a high selectivity, sensitivity and longer wavelength (700 nm) towards COX-2 expressive tumor cells.

The results showed that NB-C6-CCB has emitted strong fluorescence in MCF-7 and Hela cells (cancer cell lines) within the short time because of high levels of COX-2, whereas very less fluorescence is emitted in normal cells due to the absence of COX-2. Subcellular localization of the NB-C6-CCB has preferentially characterized the Golgi apparatus which is a rapid and sensitive factor to enhance the diagnosis effect of therapeutic cancers. NB-C6-CCB has a specific and sensitive near infrared fluorescence discriminating response with MCF-7 *versus* COS-7 in the same culture dish, confirmed by confocal microscope.

2 Experimental

2.1 Materials and methods

Solvents and reagents were used without further purification. The NB-C6-CCB solution was prepared in dimethyl sulphoxide (DMSO) at a 5 mmol/L concentration as the final stock solution. ^{1}H NMR and ^{13}C NMR spectra were recorded on a Bruker Avance II 400 MHz spectrometer. Chemical shifts (δ) were stated as ppm (in DMSO-d_6 or $CDCl_3$, with TMS as the internal standard). Mass spectrometric data were acquired by using TOF-MS instruments. Absorption intensity spectra were carried out by a Cary 60 UV-V spectrophotometer (Agilent technologies, USA). Fluorescence intensity spectra were acquired by a Cary Eclipse fluorescence spectrophotometer (Agilent technologies, USA). The absolute fluorescence quantum yields of NB-C6-CCB in different solutions were determined by Quanturus-QY (HAMAMATSU, Japan). Excitation and emission slit widths were altered and the fluorescence intensity was adjusted to a suitable wavelength range. NBD-C6-ceramide (green) and Hoechst 33342 (blue) were purchased from Life Technologies Co. (USA). Frozen tissue slices were prepared by Leica CM1860 UV (Germany).

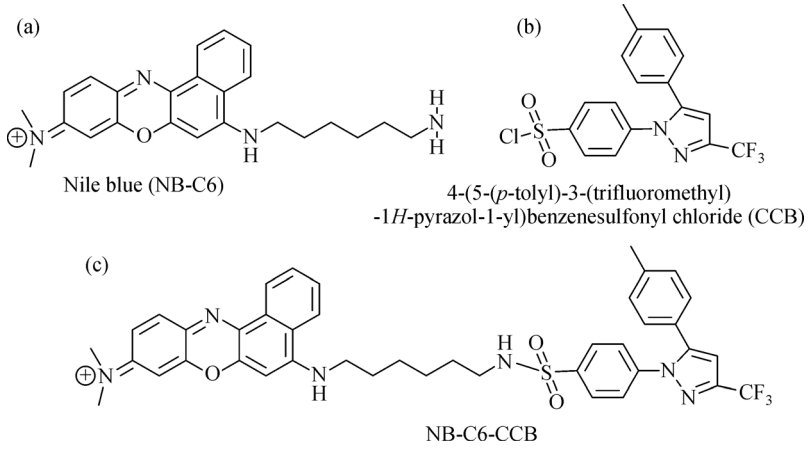

Fig. 1 Chemical structures of NB-C6-CCB. (a) NB, (b) CCB derivative (CCB) and (c) NB-C6-CCB

2.2 Synthesis of NB (step-a)

Compound **1** was synthesized from 3-(dimethylamino) phenol by the literature procedure [39].

2.3 Synthesis of NB-C6 (step-b)

NB-C6 was synthesized from the reaction of 1-bromo-naphthalene with 1,6-diaminohexane according to the reported procedure [8]. Compound **1** (1.5 g, 4.31 mmol) was dissolved in ethanol (15 mL) in an ice bath (0°C). 3-(Dimethylamino) phenol (984 mg, 6.47 mmol) and concentrated hydrochloride acid (1.0 mL) were added. The mixture was stirred for 15 min, then refluxed at 90°C for 4.5 h and monitored by TLC (CH_2Cl_2:CH_3OH = 10:1). The crude NB-C6 was obtained by recrystallization from ethanol, and then further purified by silica gel column chromatography with CH_2Cl_2/CH_3OH (6/1) to give NB-C6 as a violet solid (500 mg, 30%). ^{1}H NMR (400 MHz, CD_3OD, δ ppm): 8.86 (s, J = 8 Hz, 1H), 8.79 (d, J = 8 Hz, 1H), 8.10 (s , J = 8Hz, 2H), 7.96 (t, J = 8 Hz , 1H), 7.85 (t, J = 8 Hz , 1H), 7.24 (s, 1H), 7.06 (s, J = 8 Hz, 1H), 6.87 (s, J = 8 Hz, 1H), 3.76 (t, J = 4 Hz, 1H), 3.17 (m, 2H), 2.78 (d, J = 8 Hz, 3H), 1.78–1.23(m, 11H); ^{13}C NMR (100 MHz, CD_3OD, δ ppm): 147.38, 132.04, 132.94, 130.73, 129.75, 124.36, 123.90, 95.90, 93.83, 54.89, 45.25, 40.53, 38.50, 33.97, 28.13, 26.77, 25.79, 25.47, 8.37. HRMS: calculated for $C_{24}H_{29}N_4O^+$ $[M]^+$ 389.2336, found 389.2335.

2.4 Synthesis of NB-C6-CCB (step-c)

To a flask (100 mL) containing a solution of NB-C6 (300 mg, 770.17 μmol) in THF (15 mL), CCB (463 mg, 1.16 mmol) was added slowly at 25°C, and then triethylamine (1 mL) was added dropwise. The resulting mixture was stirred for 4 h at room temperature, and monitored by TLC (CH_2Cl_2:CH_3OH = 10:2). After reaction, the mixture was purified by neutral silica gel column chromatography eluted with CH_2Cl_2/CH_3OH (10/1 to 10/3) and NB-C6-CCB was obtained as a violet solid (200 mg, 35.15%). ^{1}H NMR (400 MHz, CD_3OD, δ ppm): 8.40 (d, J = 8 Hz, 1H), 8.01 (d, J = 8 Hz, 1H), 7.74 (d, J = 8Hz, 2H), 7.65 (t, J = 8 Hz, 1H), 7.75 (t, J = 8 Hz, 1H), 7.42 (d, 1H), 7.34 (d, J = 8 Hz, 2H), 7.22 (d, J = 8 Hz, 1H), 7.01 (q, J = 4 Hz, 5H), 6.90 (d, 1H), 6.74 (d, J = 8 Hz, 1H), 6.55 (s, J = 4 Hz, 1H), 6.40 (s, J = 8 Hz, 1H), 3.51 (t, J = 8 Hz, 2H), 3.06 (s, J = 8 Hz , 6H), 2.12 (s, J = 8 Hz, 2H), 2.16 (d, J = 8 Hz, 4H), 1.71–1.23(m, 7H); ^{13}C NMR(100 MHz, CD_3OD, δ ppm): 159.31, 157.02, 152.86, 148.90, 146.98, 145.03, 144.73, 143.55, 142.22, 141.82, 140.78, 135.23, 133.57, 132.98, 132.30, 131.03, 130.59, 129.94, 129.06, 128.06, 127.14, 126.53, 125.5, 123.86, 121.62, 116.28, 106.94, 106.52, 97.11, 94.59, 45.85, 43.86, 41.12, 30.46, 29.62, 27.38, 27.18, 21.30, 21.28. HRMS: calculated for $C_{41}H_{40}F_3N_6O_3S^+$ $[M]^+$ 753.2829, found 753.2824.

2.5 Photophysical properties of NB-C6-CCB

The absolute fluorescence quantum yields of NB-C6-CCB were determined by absolute fluorescent quantum yield meter Quanturus-QY (HAMAMATSU, Japan).

2.6 Cell incubation and staining with NB-C6-CCB

The live MCF-7 cells MDA-MB-231 (human breast cancer cells), HeLa (Human cervical cancer cells), COS-7 (African green monkey kidney cells) and HL-7702 (human normal liver cells) were bought from the Institute of Basic Medical Sciences of the Chinese Academy of Medical Sciences. Cells were incubated or cultured in 10% fetal bovine serum medium with 1% streptomycin and penicillin. The live cells were planted in 24-well flat-bottomed dishes and incubated for 24 h at 37°C under the 5% CO_2. The live cells were stained with 2.5 μmol/L of the NB-C6-CCB for another 10 min and then washed with phosphate-buffered saline (PBS) twice. Fluorescence cell imaging was achieved using an OLYMPUSFV-1000 inverted fluorescence microscope with a 60 × objective lens. The NB-C6-CCB stained images were obtained by using the excitation and emission wavelengths at 630 nm and 655–755 nm, respectively.

2.7 Native-PAGE

MCF-7 cells were stained with NB-C6-CCB at different concentrations (0, 2.5, 5.0, 10.0 μmol/L) for 30 min at 37°C, under the 5% of CO_2. After trypsinization, the cells fell out from the culture flask, and different concentrations of protein extracts were obtained by centrifugation. Add 25 μL of the 5 × native-PAGE buffers (0.2 mol/L Tris, 40% glycerol, and 0.4% bromophenol blue) into a protein sample (100 μL) for gel electrophoresis. The bands were stained with Coomassie blue, and the protein bands labeled by NB-C6-CCB were also visualized using a Night-OWL II LB983 small animal *in vivo* imaging system with a delicate charge coupled device camera. Wavelengths at 630 nm of excitation and at 700 nm of emission were used for NB-C6-CCB [26].

2.8 Fluorescence images of live cells co-stained with Golgi and nucleolus tracker

After NB-C6-CCB (2.5 μmol/L) was added to cells, NBD-C6-ceramide (Golgi-tracker, 2.5 μmol/L) and Hoechst 33342 (nucleolus tracker, 2.5 μmol/L) were used to co-stain the cells. Cells were incubated for 20 min at 37°C under 5% CO_2 and then washed with PBS three times. Fluorescence images were obtained by using OLYMPUSFV-1000 inverted fluorescence microscope with a 60 × objective lens. NB-C6-CCB (red channel), NBD-C6-ceramide (green channel), and Hoechst 33342 (blue channel) were excited at 630, 488, and 405 nm,

respectively, and their emission spectra were collected at 650–700, 500–550, 440–480 nm, respectively.

2.9 Preparation of mouse tissue slices and staining with NB-C6-CCB

Tumor tissue slices were acquired from nude tumor mouse and normal tissue slices were resected from nude mice liver. Before imaging, the tumor tissues slices were incubated with 2.5 μmol/L NB-C6-CCB for another 20 min and then washed with phosphate-buffered saline (PBS) twice. Fluorescence images were obtained as described in section 2.8.

2.10 Fluorescence imaging *in vivo*

Procedures and protocols were carried out in agreement with the Guide for the Care and Use of Laboratory Animal Resources and the National Research Council, and were approved by the Institutional Animal Care and Use of laboratory resource. Human breast cancer cell lines MCF-7 were used for *in vivo* studies. The tumor grafts were produced by the sub-skin injection of (1×10^6 to 2×10^6 concentration) of MCF-7 cells, these cells were suspended in 200 to 300 μL of PBS and then injected into BALB/c nude mice. Experiments of the tumor bearing mice were finished in 17 d, when tumor size grew up to 0.4–0.6 cm. The NB-C6-CCB (200 μmol/L/100 μL) was injected to the mice with tumor by subcutaneous injection at 2 cm away from the tumor region, and the mice were imaged after 1 h.

2.11 Flow cytometry (competition with CCB)

MDA-MB-231 cells were incubated in dulbecco's modified eagle medium (DMEM) supplemented with 10% FBS (fetal bovine serum) under 5% of CO_2 and 95% of air at 37°C. Three groups of MDA-MB-231 cells were separately (1) incubated without NB-C6-CCB as a control group, (2) stained with the NB-C6-CCB (1.0 μmol/L) for 15 min, and (3) pre-incubated with CCB (10 μmol/L or 15 μmol/L) for 2 h and then stained with 1.0 μmol/L of NB-C6-CCB for 15 min. The resulting cells were analyzed by a FAC Scan cytometer (Becton Dickinson Biosciences Pharmingen, USA), and all data were analyzed with Cell Quest software [37].

2.12 Cytotoxicity experiments

Cell viability quantities were assessed by MTT (3-(4,5)-dimethylthiahiazo (-2-yl)-3,5-diphenytetrazoliumromide) to formazan crystals were using mitochondrial dehydrogenases. MCF-7 cells were seeded in a 96-well microplate (Nunc, Denmark) at a density of 1×10^5 cells/mL (100 μL/well of the DMEM medium containing 10% FBS). The cells were incubated for 24 h, and then plates were washed three times with PBS (100 μL/well). The MCF-7 cells were stained with NB-C6-CCB (0, 2.5, 5.0, 10.0 and 15.0 μmol/L) and then medium was incubated for 24 h. The cell culture medium without NB-C6-CCB was used as a control group. Six replicate wells were measured as control and test concentration. Then MTT (10 μL, 5 mg/mL) in PBS was added to each well in the plates and incubated at 37°C for another 4 h in a 5% CO_2 humidified incubator. The medium was removed carefully, and the purple crystals were lysed in 150 μL DMSO. Optical density was determined on a microplate reader (Thermo Fisher Scientific) at 570 nm with subtraction of the absorbance of the cell-free blank volume at 630 nm [41].

3 Results and discussion

3.1 Spectral properties of NB-C6-CCB and response to COX-2

The synthesis of NB-C6-CCB is shown in Scheme 1 and the intermediates were well characterized by ^{1}H-NMR, ^{13}C-NMR and ESI-HRMS (see the Electronic Supplementary Material S3–S8). The intensity profile of NB-C6-CCB in different solvents and the corresponding quantum yields were depicted in Electronic Supplementary Material (see the Fig. S1 and Table S1).

The "off-on" mechanism of the fluorescent probe depends on the length of carbon linker between probe (signaling group) and inhibitor (receptor group). A six-carbon linker enhances fluorescence compared with a two- or eight-carbon linker in the present case. Hence, we select a six-carbon linker for probe (NB-C6-CCB) designing and we assume the six carbon linker of NB-C6-CCB may have off-on mechanism with COX-2.

NB-C6-CCB (λ_{ex} = 630 nm) shows very weak fluorescence in aqueous buffer solution. However, the fluorescence is restored when NB-C6-CCB interacts with COX-2 in cancer cells (MCF-7 or HeLa), because CCB binds strongly to COX-2 side pocket of three amino acids (Val523, Arg513 and Val434) [35]. It has been reported that the IC_{50} values for CCB are 0.4 μmol/L and 0.35 mmol/L [33,34].

Enzyme-linked immune sorbent assays showed that cancer cells express high level of COX-2 enzymes, such as HT-29 (2.467 μg/mL), HeLa (2.13 μg/mL), MCF-7 (3.758 μg/mL), and tumour tissues (4.52 μg/mL), but COX-2 expresses at low levels in HCT-116 cancer cells (0.00075 μg/mL) and normal cells (HL-7702 cell 0.00094 μg/mL, COS-7 cell 0.0077 μg/mL). Normal tissues (0.0056 μg/mL) have similar results as reported in our group [19].

3.2 Strategy of COX-2 selective near infrared fluorescent probe

Native polyacrylamide gel electrophoresis (Native-PAGE)

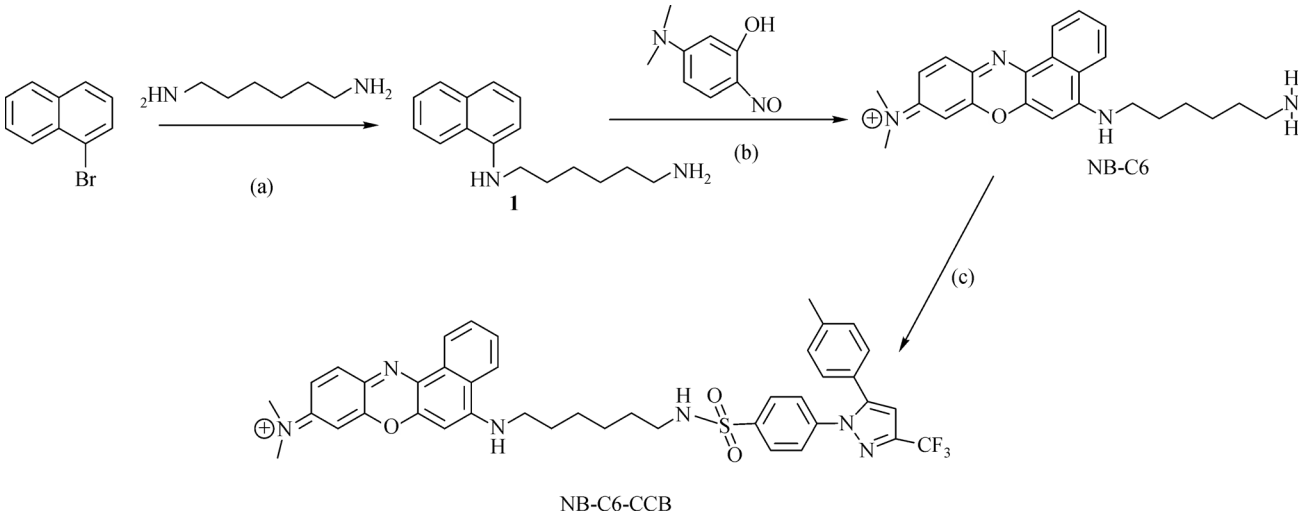

Scheme 1 Synthesis of NB-C6-CCB. Reagents and conditions: (a) methoxyethanol, CuI, $CsCO_3$, 125°C, 24 h, (b) ethanol, HCl, 90°C, 4.5 h, (c) THF, CCB derivative, TEA, 4 h, r.t.

analysis was used to investigate whether the NB-C6-CCB exactly binds to purified COX-2 enzyme. Cancer cell lines (MCF-7) were stained with NB-C6-CCB (0, 2.5, 5.0, 10.0 μmol/L) for 30 min, the fluorescence emission bands were detected in gel holding purified COX-2 (Fig. 2(b)). Moreover, the fluorescence intensity depends on the concentration of the probe in samples. This experiment indicates that NB-C6-CCB perfectly binds to COX-2 enzyme, and can thus be used as a perfect bio-marker to COX-2 in biological samples.

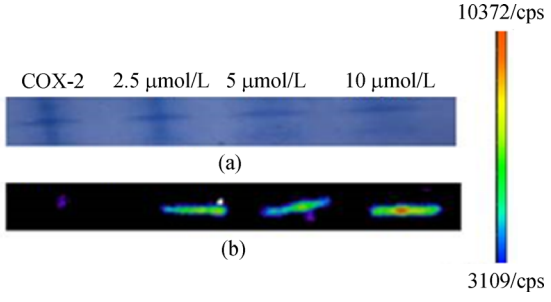

Fig. 2 Native-PAGE analysis of NB-C6-CCB labeling. (a) Coomassie brilliant blue staining, (b) fluorescence image with excitation 630 nm and emission wavelengths 640–700 nm (lane 1: purified cyclooxygenases-2; lanes 2–4: protein extracts of MCF-7 cells incubated with various concentrations of NB-C6-CCB for 30 min)

3.3 Fluorescence discrimination of cancer cells from normal cells

Normal cells (COS-7, HL-7702) express low fluorescence due to less amount of COX-2 (Fig. 3). NB-C6-CCB probe interaction or fluorescence intensity with COX-2 depends on the amount of COX-2 presented in the cancer cell lines (Fig. 3(e)), because the CCB moiety binds strongly to COX-2 side pocket of three amino acids (Val523, Arg513 andVal434) in the cancer cells. Hence the NB-C6-CCB showed strong fluorescence intensity in COX-2 expressed cancer cells. Accordingly, prolonged irradiation of the laser light (emission: 640–700 nm) about 0–120 min, illustrated that NB-C6-CCB has excellent photostability in living cells (see the Figs. S2(a–c)).

3.4 Fluorescence discrimination of cancer cells in co-culture dish (MCF-7 and COS-7)

The live cells (MCF-7 and COS-7) were co-cultured and stained with NB-C6-CCB (2.5 μmol/L) for 10 min. All images were acquired by using the excitation and emission windows of λ_{ex} = 635 nm and λ_{em} = 640–700 nm. Cancer cell lines (MCF-7) expressed stronger fluorescence than normal cells (COS-7) with NB-C6-CCB, even in single culture medium (Fig. 4). Confocal imaging of single culture medium (MCF-7 and COS-7), showed the selectivity of NB-C6-CCB towards COX-2 with subcellular localization.

3.5 Selectivity confirmation with CCB-competition

For the selectivity confirmation of NB-C6-CCB, COX-2 expressed cells (MCF-7 and HeLa cells) (Figs. 5(A,B)) were pre-incubated with CCB 0, 5, 10 μmol/L for 3 h, and then NB-C6-CCB (1.0 μmol/L) was added. As shown in Figs. 5(C,D)), the fluorescence intensity was inhibited by the increasing concentration of CCB, indicating that NB-C6-CCB has excellent binding towards COX-2 enzyme moiety.

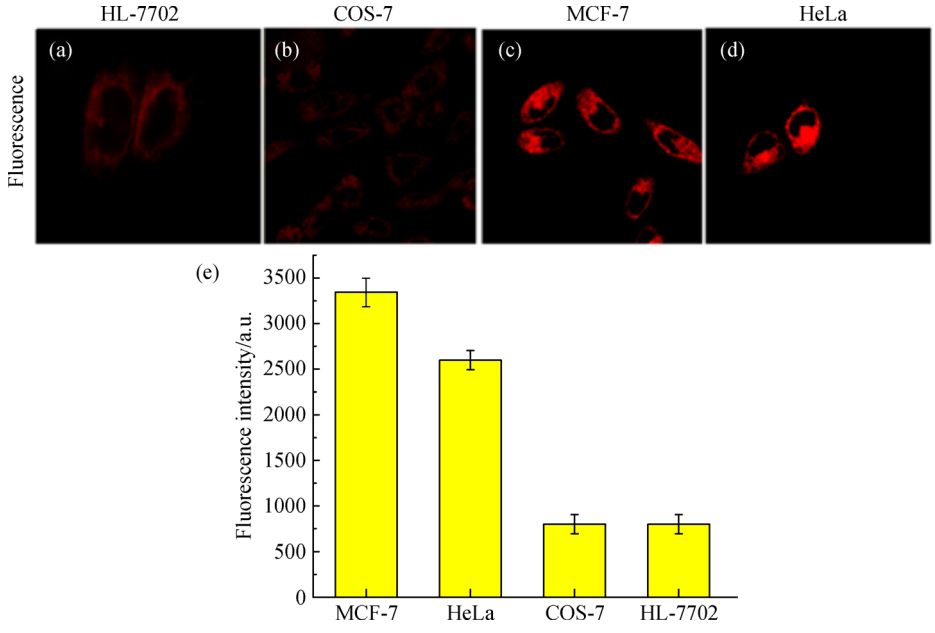

Fig. 3 Fluorescent images of live cells stained with NB-C6-CCB (2.5 μmol/L). (a) HL-7702, (b) COS-7, (c) MCF-7, (d) HeLa and (e) fluorescence intensity of live cells (λ_{ex} = 630 nm, λ_{em} = 640−700 nm)

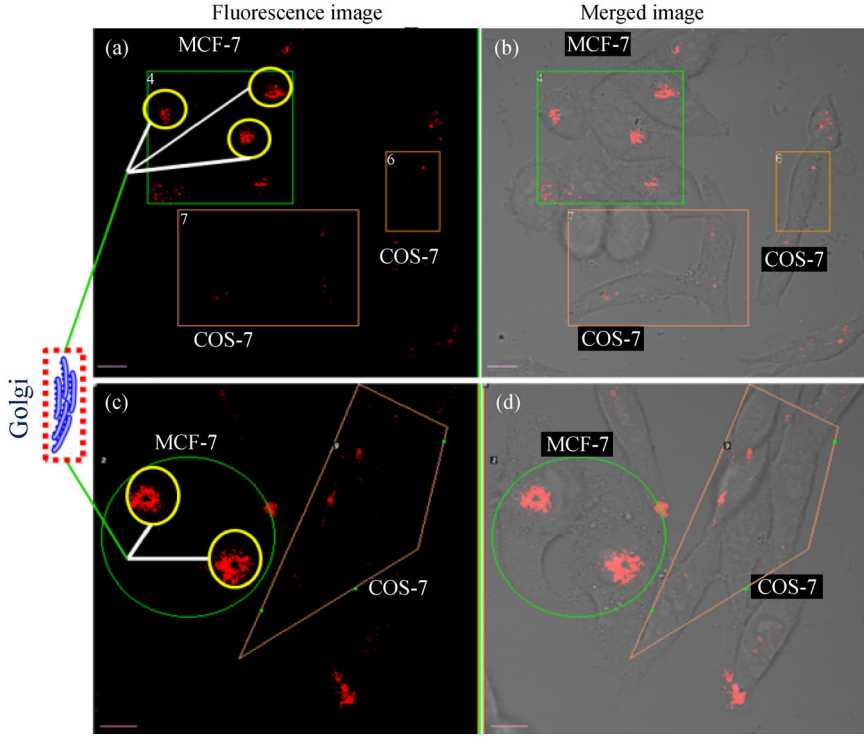

Fig. 4 Normal and cancer cells co-cultured and stained with NB-C6-CCB (2.5 μmol/L). (a) and (c) Fluorescence of co-cultured cancer (MCF-7) and normal cells (COS-7), (b) and (d) overly of co-cultured cancer (MCF-7) and normal cells (COS-7). Images were acquired by confocal microscopy (λ_{ex} = 630 nm, scan range λ_{em} = 640−700 nm)

3.6 CCB competition experiments by flow cytometry

MDA-MB-231 cells were pre-incubated with CCB (10 or 15 μmol/L) for 30 min or 1.5 h, then NB-C6-CCB (1.0 μmol/L) was added and analyzed by flow cytometry. The result shows the fluorescence intensity background decreases with increasing CCB pre-incubation time and concentration. As shown in Fig. 6, only MDA-MB-231

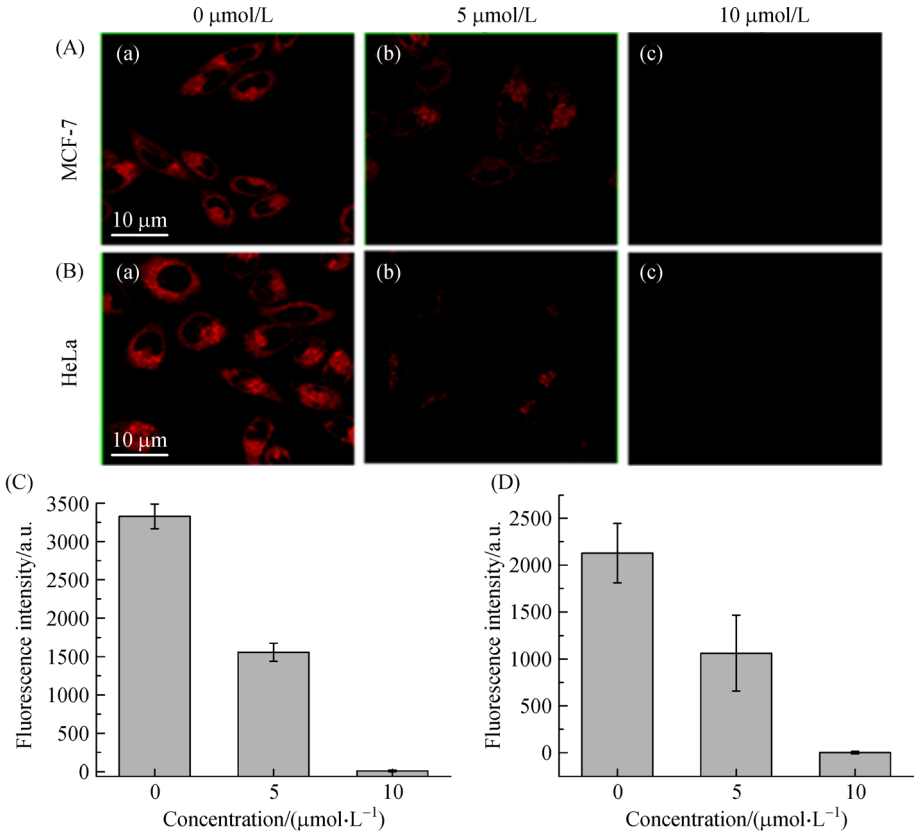

Fig. 5 Selectivity conformation of NB-C6-CCB. (A) MCF-7 and (B) HeLa were pre-incubated with CCB 0, 5, 10 μmol/L for 3 h and then 1.0 μmol/L of NB-C6-CCB was added. λ_{ex} = 630 nm, scan range λ_{em} = 640−700 nm; quantitative image analysis of the average total fluorescence of (C) MCF-7 cells and (D) HeLa cells

cells containing NB-C6-CCB shows high fluorescence intensity (Fig. 6). The flow cytometry experiments demonstrated that, NB-C6-CCB was a good COX-2 recognizing agent and showed the sensitivity towards COX-2 over-expressed cancer cells.

3.7 Golgi and hoechst 33342 co-localization

NBD-C6-Ceramide was the bright probe for Golgi localization. The maximum COX-2 enzymes were expressed in Golgi complex, so that we selected commercial NBD-C6-Ceramide for the comparison. NB-C6-CCB (2.5 μmol/L) and NBD-C6-Ceramide (2.5 μmol/L) were co-stained in MDA-MB-231 cells. The co-localization co-efficients were assessed by Pearson's co-relation factors [42]. As shown in Fig. 7, NB-C6-CCB (Fig. 7(b)) and NBD-C6-Ceramide (Fig. 7(a)) were localized at Golgi complex in MDA-MB-231 cells (Fig. 7 (c)) with cross co-stain intensity profile (Fig. 7(e)), Pearson's co-relation factor is 0.94 (Fig. 7(f)), indicating that both probes combine perfectly and NB-C6-CCB is mostly localized in Golgi complex of cancer cells. Similarly, hoechst 33342 has been used as an outstanding nucleolus tracker [43]. Thus, NB-C6-CCB (2.5 μmol/L), NBD-C6-ceramide (2.5 μmol/L) and Hoechst 33342 (2.5 μmol/L) were multi-stained in MDA-MB-231 cells, showing that NB-C6-CCB has not merged perfectly with DNA tracker like NBD-C6-ceramide as co-localization shows (Fig. 8).

3.8 Fluorescence imaging of mice tissue slices

The mouse breast cancer tissue and normal liver tissue from nude mouse were incubated with NB-C6-CCB (2.5 μmol/L) for 20 min. As shown in Fig. 9, the breast cancer tissue slices (Fig. 9(A)) exhibit high fluorescence with deeper penetration into tissue (depth: 500 μm), as specifically shown in 3D image (Fig. 9(B(c))), whereas normal liver tissue (Fig. 9(C)) show very less fluorescence due to different concentrations of level of COX-2. Because inflammation tissues always contain COX-2 to some extent [19], unfortunately, the probe could not distinguish cancer from inflammation tissues although cancer tissues show much brighter fluorescence.

3.9 Fluorescence imaging in tumor mice

NB-C6-CCB (40 μmol/L) was dissolved in PBS (100 μL) and then injected to tumor mouse (MCF-7) by tail vein injection. As shown in Fig. 10, the tumor part of MCF-7

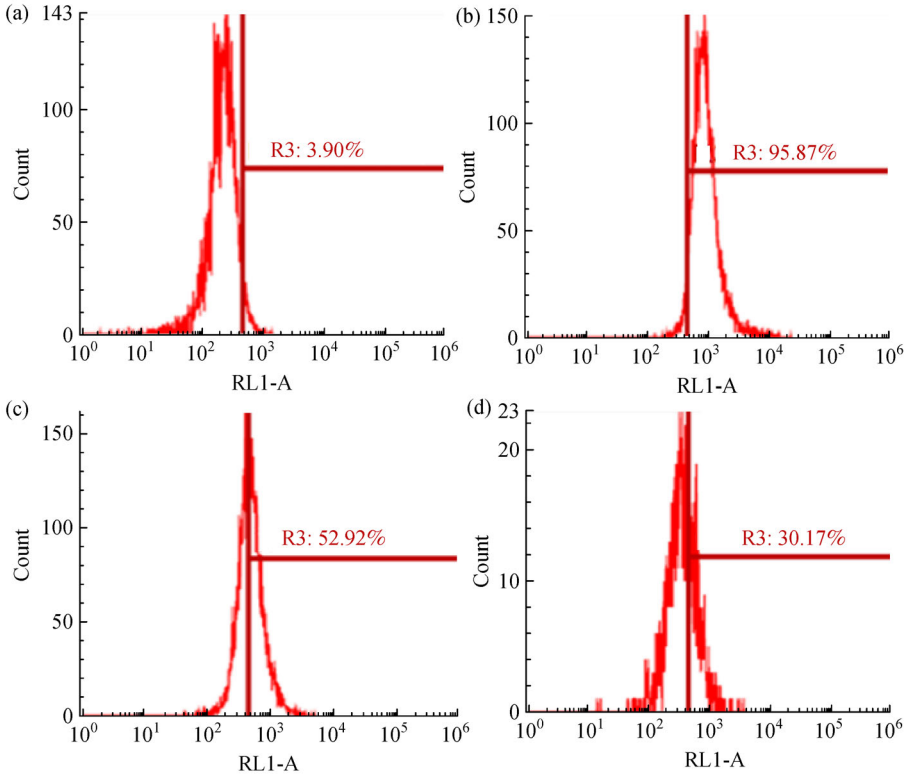

Fig. 6 Flow cytometry analysis of competition of CCB with NB-C6-CCB for COX-2 in MDA-MB-231 cells. (a) Control group, (b) stained with only NB-C6-CCB (1.0 μmol/L), (c) pre-incubated with CCB 10 μmol/L for 2.0 h and then added 1.0 μmol/L of NB-C6-CCB, (d) pre-incubated with CCB 15 μmol/L for 2.0 h and then added 1.0 μmol/L of NB-C6-CCB (λ_{ex} = 630 nm, scan range λ_{em} = 640−700 nm)

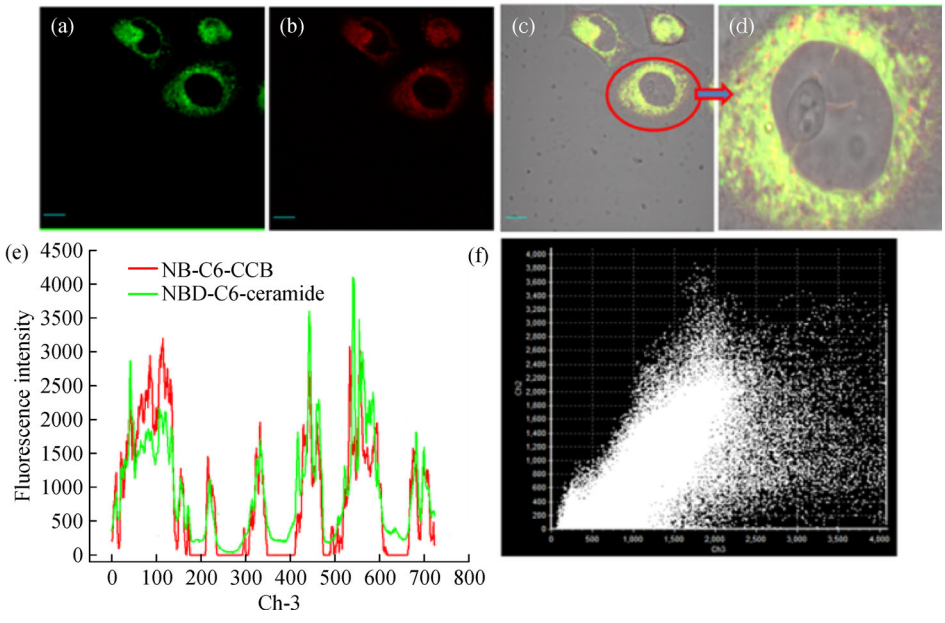

Fig. 7 Fluorescence images of NB-C6-CCB (2.5 μmol/L) co-stained with NBD-C6-Ceramide (2.5 μmol/L) in MDA-MB-231 cells. (a) Green emission of Golgi tracker (λ_{ex} = 488 nm, λ_{em} = 500−540 nm), (b) red emission of NB-C6-CCB (λ_{ex} = 630 nm, λ_{em} = 640−700 nm), (c) overlay of the green and red channels, (d) overlay zoom image from picture c, (e) intensity profile of cross co-stain image, (f) Pearson's co-efficient graph of overlay

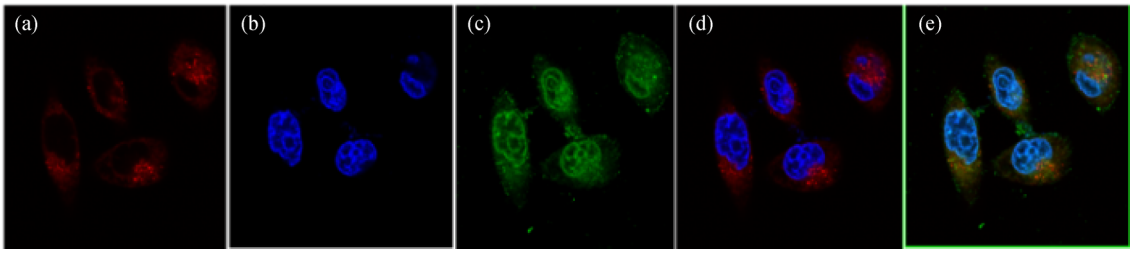

Fig. 8 Fluorescence images of NB-C6-CCB (2.5 µmol/L) co-stained with NBD-C6-ceramide (2.5 µmol/L) and Hoechst 33342 (2.5 µmol/L) in MDA-MB-231 cells. (a) Red emission of NB-C6-CCB (λ_{ex} = 630 nm, λ_{em} = 640−700 nm), (b) blue emission of Hoechst 33342 (λ_{ex} = 405 nm, λ_{em} = 440−480 nm), (c) green emission of Golgi tracker (λ_{ex} = 488 nm, λ_{em} = 500−540 nm), (d) overlay of the blue and red channels, (e) overlay of NB-C6-CCB, hoechst 33342 and NBD-C6-ceramide

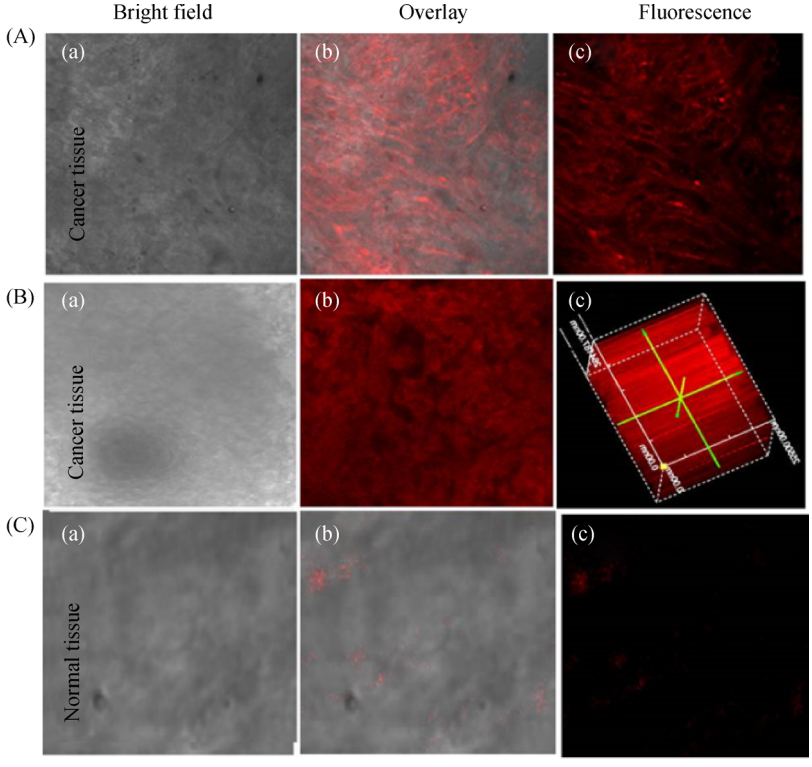

Fig. 9 Fluorescence imaging of cancer and normal tissues with stained NB-C6-CCB (2.0 µmol/L). A(a) bright field, A(b) merged, A(c) fluorescence image; B(a) bright field, B(b) 2D image, B(c) 3D images of tumor tissue (length: 500 µm); C(a) bright field, C(b) merged, C(c) fluorescence images of normal mouse liver tissue

visualized shows strong fluorescence intensity at exact place of tumor region (Fig. 10A(b)), and then from the same tumor mouse, we resected the tumor lump, liver, heart, kidney, and spleen (Fig. 10(B)). The NB-C6-CCB fluorescence intensity is still strong in the tumor lump (Fig. 10B(a)) and there is no fluorescence indication in normal mice organs.

3.10 Cytotoxicity

The MTT assay proved that NB-C6-CCB has no cytotoxicity towards living cells and stimulates the cell proliferation (Fig. 11). Consequently, NB-C6-CCB has no

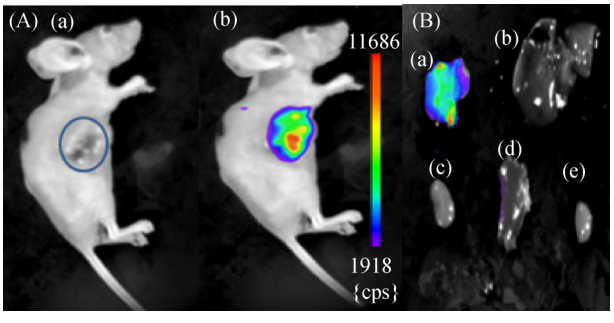

Fig. 10 Fluorescence imaging of tumor mouse and organs by using NB-C6-CCB. A(a) white light, A(b) merged light; B(a) tumor lump, B(b) liver, B(c) kidney, B(d) spleen, B(e) heart

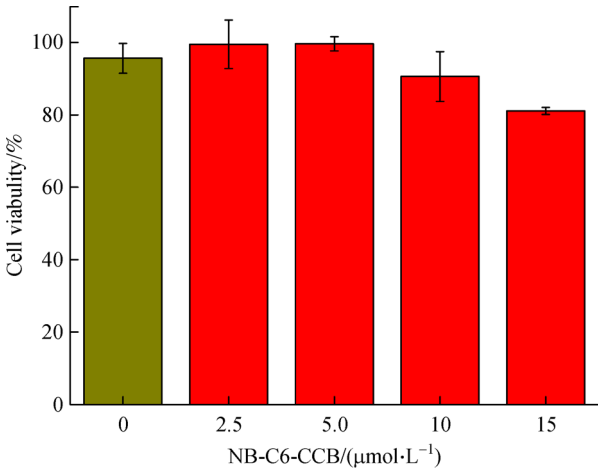

Fig. 11 MTT assay of NB-C6-CCB in live cells (MCF-7)

toxicity between the concentrations of 2.5 to 15 μmol/L. Therefore, we suggest NB-C6-CCB could be used for further studies.

4 Conclusions

We have demonstrated that COX-2 is hyperactive and Golgi is localized near-infrared fluorescent probe (NB-C6-CCB), and by using this probe, the cancer cell lines can be discriminated from normal cells in terms of the intensity and localization (Golgi localization) due to the differentiate level of COX-2. NB-C6-CCB exhibits strong fluorescence (λ_{em} = 640–700 nm) in the presence of cancer cells, because the inhibitor moiety binds strongly to the COX-2 amino acid pockets. Importantly, subcellular localization of the NB-C6-CCB particularly indicates in the Golgi apparatus and enhances the fluorescence intensity in Golgi, mostly in the COX-2 expressed cancer cells. Interestingly, confocal laser microscopy imaging, CCB-competition imaging and native-PAGE proved the selectivity of NB-C6-CCB to COX-2. The NB-C6-CCB probe penetrates deeper towards tumor tissue, which was confirmed by 3D imaging. Remarkably, *in vivo* experiments of tumor mouse and organs show the excellent NIR visualization on particular part of the tumor with high fluorescence intensity. MTT analysis results show that NB-C6-CCB is not harmful to living cells. Therefore, NB-C6-CCB is an excellent tool for COX-2 imaging in the tumor with long wavelength (λ_{em} = 700 nm) without the disturbance of normal cells or tissues.

Acknowledgements This work was financially supported by the National Natural Science Foundation of China (Grant Nos. 21421005, U1608222 and 21576037).

Electronic Supplementary Material Supplementary material is available in the online version of this article at https://doi.org/10.1007/s11705-019-1796-1 and is accessible for authorized users.

References

1. Fass L. Imaging and cancer. Molecular Oncology, 2008, 2(2): 115–152
2. Nguyen Q T, Olson E S, Aguilera T A, Jiang T, Scadeng M, Ellies L G, Tsien R Y. Surgery with molecular fluorescence imaging using activatable cell-penetrating peptides decreases residual cancer and improves survival. Proceedings of the National Academy of Sciences of the United States of America, 2010, 107(9): 4317–4322
3. De Vries E F, Doorduin J, Dierckx R A, van Waarde A. Evaluation of [(11)C]rofecoxib as PET tracer for cyclooxygenase 2 over-expression in rat models of inflammation. Nuclear Medicine and Biology, 2008, 35(1): 35–42
4. Wang Z, Gao H, Zhang Y, Liu G, Niu G, Chen X. Functional ferritin nanoparticles for biomedical applications. Frontiers of Chemical Science and Engineering, 2017, 11(4): 633–646
5. Yukawa H, Baba Y. *In vivo* fluorescence imaging and the diagnosis of stem cells using quantum dots for regenerative medicine. ACS Analytical Chemistry, 2017, 89(5): 2671–2681
6. Belloch J P, Rovira V, Llacer J L, Riesgo P A, Cremades A. Fluorescence-guided surgery in high grade gliomas using an exoscope system. Acta Neurochirurgica, 2014, 156(4): 653–660
7. Stummer W, Reulen H J, Meinel T, Pichlmeier U, Schumacher W, Tonn J C, Rohde V, Oppel F, Turowski B, Woiciechowsky C, et al. Extent of resection and survival on glioblastoma multiforme-identification of and adiustment for bias. Neurosurgery, 2008, 62(3): 564–574
8. Wang B, Fan J, Wang X, Zhu H, Wang J, Mu H, Peng X. A nile blue based infrared fluorescent probe: Imaging tumors that over-express cyclooxygenase-2. RSC Chemical Communication, 2015, 51(4): 792–795
9. Lin C W, Shulok J R, Kirley S D, Cincotta L, Foley J W. Lysosomal localization and mechanism of uptake of nile blue photosensitizers in tumor cells. Cancer Research, 1991, 51: 2710–2719
10. Mao Z, Feng W, Li Z, Zeng L, Lv W, Liu Z. NIR in, far-red out: Developing a two-photon fluorescent probe for tracking nitric oxide in deep tissue. RSC Chemical Science, 2016, 7(8): 5230–5235
11. Mao Z, Jiang H, Song X, Hu W, Liu Z. Development of a silicon-rhodamine based near-infrared emissive two-photon fluorescent probe for nitric oxide. ACS Analytical Chemistry, 2017, 89(18): 9620–9624
12. Luchsinger C, Aguilar M, Burgos P V, Ehrenfeld P, Mardones G A. Functional disruption of the Golgi apparatus protein ARF1 sensitizes MDA-MB-231 breast cancer cells to the antitumor drugs actinomycin D and vinblastine through ERK and AKT signaling. PLoS One, 2018, 13(4): 1–25
13. Wlodkowic D, Skommer J, McGuinness D, Hillier C, Darzynkiewicz Z. ER-Golgi network—a future target for anti-cancer therapy. Leukemia Research, 2009, 33(11): 1440–1447
14. Sakhrani N M, Padh H. Organelle targeting: Third level of drug targeting. Drug Design, Development and Therapy, 2013, 7: 585–599
15. Migita T, Inoue S. Implications of the Golgi apparatus in prostate cancer. International Journal of Biochemistry & Cell Biology, 2012,

44(11): 1872–1876
16. Korkmaz C G, Korkmaz K S, Kurys P, Elbi C, Wang L, Klokk T I, Hammarstrom C, Troen G, Svindland A, Hager G L, Saatcioglu F. Molecular cloning and characterization of STAMP2, an androgen-regulated six transmembrane protein that is overexpressed in prostate cancer. Oncogene, 2005, 24(31): 4934–4945
17. Uddin M J, Crews B C, Blobaum A L, Kingsley P J, Gorden D L, McIntyre J O, Matrisian L M, Subbaramaiah K, Dannenberg A J, Piston D W, Marnett L J. Selective visualization of cyclooxygenase-2 in inflammation and cancer by targeted fluorescent imaging agents. Cancer Research, 2010, 70(9): 3618–3627
18. Uddin M J, Crews B C, Huda I, Ghebreselasie K, Daniel C K, Marnett L J. Trifluoromethyl fluorocoxib a detects cyclooxygenase-2 expression in inflammatory tissues and human tumor xenografts. ACS Medicinal Chemistry Letters, 2014, 5(4): 446–450
19. Zhang H, Fan J, Wang J, Dou B, Zhou F, Cao J, Qu J, Cao Z, Zhao W, Peng X. Fluorescence discrimination of cancer from inflammation by molecular response to COX-2 enzymes. Journal of the American Chemical Society, 2013, 135(46): 17469–17475
20. Keereweer S, Van Driel P B, Robinson D J, Lowik C W. Shifting focus in optical image-guided cancer therapy. Molecular Imaging & Biology, 2014, 16(1): 1–9
21. Tian J, Yan Q, Zhu Y, Zhang J, Li J, Shi B, Xu G, Fan C, Zhao C. Enzyme-triggered fluorescence turn-on: A probe for specifically imaging ovarian-cancer-related γ-glutamyltranspeptidase. Chinese Journal of Chemistry, 2017, 35(11): 1711–1716
22. Sedgwick A C, Hayden A, Hill B, Bull S D, Elmes R B P, James T D. A simple umbelliferone based fluorescent probe for the detection of nitroreductase. Frontiers of Chemical Science and Engineering, 2018, 12(2): 311–331
23. Gu K, Xu Y, Li H, Guo Z, Zhu S, Zhu S, Shi P, James T D, Tian H, Zhu W H. Real-time tracking and *in vivo* visualization of *β*-galactosidase activity in colorectal tumor with a ratiometric near-infrared fluorescent probe. Journal of the American Chemical Society, 2016, 138(16): 5334–5340
24. Minchew C L, Didenko V V. Fluorescent probes detecting the phagocytic phase of apoptosis: Enzyme-substrate complexes of topoisomerase and DNA. Molecules (Basel, Switzerland), 2011, 16 (6): 4599–4614
25. Zhang H, Fan J, Wang J, Zhang S, Dou B, Peng X. An off-on COX-2-specific fluorescent probe: Targeting the Golgi apparatus of cancer cells. Journal of the American Chemical Society, 2013, 135(31): 11663–11669
26. Gurram B, Zhang S, Li M, Li H, Xie Y, Cui H, Du J, Fan J, Wang J, Peng X. CCB conjugated fluorescent probe for identification and discrimination of cyclooxygenase-2 enzyme in cancer cells. ACS Analytical Chemistry, 2018, 90(8): 5187–5193
27. Fan J, Guo S, Wang S, Kang Y, Yao Q, Wang J, Gao X, Wang H, Du J, Peng X. Lighting-up breast cancer cells by a near-infrared fluorescent probe based on KIAA1363 enzyme-targeting. RSC Chemical Communication, 2017, 53(35): 4857–4860
28. Guo S, Fan J, Wang B, Xiao M, Li Y, Du J, Peng X. Highly selective red-emitting fluorescent probe for imaging cancer cells *in situ* by targeting pim-1 kinase. ACS Applied Materials & Interfaces, 2018, 10(2): 1499–1507
29. Soslow R A, Dannenberg A J, Rush D, Woerner B M, Khan K N, Masferrer J, Koki A T. COX-2 is expressed in human pulmonary, colonic and mammary tumors. Cancer, 2000, 89(12): 2637–2645
30. Richardsen E, Uglehus R D, Due J, Busch C, Busund L T. COX-2 is overexpressed in primary prostate cancer with metastatic potential and may predict survival. A comparison study between COX-2, TGF-β, IL-10 and Ki67. Cancer Epidemiology, 2010, 34(3): 316–322
31. Mrena J, Wiksten J P, Kokkola A, Nordling S, Ristimaki A, Haglund C. COX-2 is associated with proliferation and apoptosis markers and serves as an independent prognostic factor in gastric cancer. Tumour Biology, 2010, 31(1): 1–7
32. Rizzo M T. Cyclooxygenase-2 in oncogenesis. Clinica Chimica Acta, 2011, 412(9-10): 671–687
33. Bhardwaj A, Kaur J, Sharma S K, Huang Z, Wuest F, Knaus E E. Hybrid fluorescent conjugates of COX-2 inhibitors: Search for a COX-2 isozyme imaging cancer biomarker. Bioorganic & Medicinal Chemistry Letters, 2013, 23(1): 163–168
34. Bhardwaj A, Kaur J, Wuest F, Knaus E E. Fluorophore-labeled cyclooxygenase-2 inhibitors for the imaging of cyclooxygenase-2 overexpression in cancer: Synthesis and biological studies. ChemMedChem, 2014, 9(1): 109–116, 240
35. Hood W F, Gierse J K, Isakson P C, Kiefer J R, Kurumbail R G, Seibert K, Monahan J B. Characterization of CCB and valdecoxib binding to cyclooxygenase. Molecular Pharmacology, 2003, 63(4): 870–877
36. Davis T W, O'Neal J M, Pagel M D, Zweifel B S, Mehta P P, Heuvelman D M, Masferrer J L. Synergy between CCB and radiotherapy results from inhibition of cyclooxygenase-2-derived prostaglandin E2, a survival factor for tumor and associated vasculature. Cancer Research, 2004, 64(1): 279–285
37. Shao D, Kan M, Qiao P, Pan Y, Wang Z, Xiao X, Li J, Chen L. CCB induces apoptosis via a mitochondriadependent pathway in the H22 mouse hepatoma cell line. Molecular Medicine Reports, 2014, 10 (4): 2093–2098
38. Xie S Q, Zhang Y H, Li Q, Wang J H, Li J H, Zhao J, Wang C J. COX-2-independent induction of apoptosis by CCB and polyamine naphthalimide conjugate mediated by polyamine depression in colorectal cancer cell lines. International Journal of Colorectal Disease, 2012, 27(7): 861–868
39. Hu M, Fan J, Li H, Song K, Wang S, Cheng G, Peng X. Fluorescent chemodosimeter for Cys/Hcy with a large absorption shift and imaging in living cells. Organic & Biomolecular Chemistry, 2011, 9 (4): 980–983
40. Li H D, Yao Q C, Fan J L, Jiang N, Wang J Y, Xia J, Peng X J. A fluorescent probe for H_2S *in vivo* with fast response and high sensitivity. RSC Chemical Communication, 2015, 51(90): 16225–16228
41. Zhu H, Fan J, Wang J, Mu H, Peng X. An "enhanced PET"-based fluorescent probe with ultrasensitivity for imaging basal and elesclomol-induced HClO in cancer cells. Journal of the American Chemical Society, 2014, 136(37): 12820–12823
42. Ahlgren P, Jarneving B, Rousseau R. Requirements for a cocitation

similarity measure, with special reference to Pearson's correlation coefficient. Journal of the American Society for Information Science and Technology, 2003, 54(6): 550–560

43. Li M, Tian R, Fan J, Du J, Long S, Peng X. A lysosome-targeted BODIPY as potential NIR photosensitizer for photodynamic therapy. Dyes and Pigments, 2017, 147: 99–105